Egyptian Journal of Aquatic Biology & Fisheries
Zoology Department, Faculty of Science,
Ain Shams University, Cairo, Egypt.
ISSN 1110 – 6131
Vol. 27 (3): 491 – 513 (2023)
www.ejabf.journals.ekb.eg

Larvicidal Efficacy of Fe-MOF Nanoparticles Against *Culex pipiens* L. (Diptera: Culicidae) and its Potential Impact on Water Quality

Omnia M. H. M. Kamel[1], M. Hamdy El Awady[2], Ahmed A. Dahaba[2], Reda M. Abdelhameed[1], Ola H. Zyaan[3, *], Shaimaa M. Farag[3]

[1]Applied Organic Chemistry Department, Institute of Industrial Chemistry Research, National Research Centre, Dokki, Giza, 12622, Egypt

[2]Water Pollution Research & Control Department, Institute of Environmental Researches & Climate Changes, National Research Centre, Dokki, Giza, 12622, Egypt

[3]Department of Entomology, Faculty of Science, Ain Shams University, Cairo, 11566, Egypt

*** Corresponding authors: ozyaan@sci.asu.edu.eg, ORCHID ID: 0000-0001-8200-3261**

ARTICLE INFO

Article History:
Received: May 30, 2023
Accepted: June 8, 2023
Online: June 11, 2023

Keywords:
Fe-MOF,
Culex pipiens,
Water quality,
Larvicides

ABSTRACT

This study investigated the potential impact of Fe-MOF (Iron Metal-Organic Framework) on wastewater treatment for disinfection purposes. The morphology, structure and composition of Fe-MOF nanoparticles were characterized using various analytical techniques, confirming their high quality and uniformity. The efficacy of Fe-MOF nanoparticles in wastewater treatment was evaluated by analyzing its physico-chemical parameters including heavy metals, in the raw and nano-treated wastewater samples under investigation. Results showed significant improvements in the quality of the treated wastewater, with removal efficiencies up to 82% for turbidity and 95% for chemical oxygen demand (COD), respectively. The study proved that Fe-MOF nanoparticles showed great potential as an effective solution for wastewater treatment and reducing the concentration of pollutants. The susceptibility of the 3rd instar larvae of *Culex pipiens* to Fe-MOF nanoparticles at different concentrations and time intervals was investigated. The mortality rate of larvae was recorded at 24, 48, and 72 hours of exposure at different concentrations of Fe-MOF nanoparticles, and the LC_{50} and LC_{95} values were determined. The LC_{50} values of Fe-MOF nanoparticles at 24, 48, and 72 hours were 93.48, 48.68, and 40.88 ppm, respectively. The LC_{95} values at 24, 48, and 72 hours were 548.23, 293.23, and 249.28 ppm, respectively. The study found that the toxicity of Fe-MOF nanoparticles on *Cx pipiens* larvae is concentration- and time-dependent. Additionally, the study focused on comparing the midgut and ovary of untreated *Cx. pipiens* with those treated with Fe-MOF nanoparticles using transmission electron microscopy (TEM). The TEM results showed significant alterations in the midgut and ovarian structures of *Cx. pipiens* larvae treated with Fe-MOF nanoparticles when compared to the untreated samples. This study showed promising results in the use of Fe-MOF nanoparticles as a promising larvicidal agent for mosquito control, thus it could contribute to integrated vector management programs. It is concluded that Fe-MOF nanoparticles exhibit very important application prospects in environmental and health-related challenges.

INTRODUTION

Polluted drainage and stagnant water spots pose a significant environmental challenge in both rural and urban areas. These polluted areas are not only affecting human health but also possess detrimental impacts on animals, plants and the overall environment **(Chowdhary *et al*., 2020)**. According to **El-Awady and Ali (2012)**, the issue of polluted areas in Egypt was exacerbated by the use of sewage sludge in agriculture, which contains high levels of contaminants. Wastewater originating from the meat processing industry was also a significant source of pollutants. To address these challenges, researchers have explored various effective treatment technologies. An advanced calcium-aluminum precipitation method effectively removed sulfate ions as well as heavy metals including Cr, Ni, Cd, Pb, Fe, Mn, and Zn from industrial wastewater **(El-Awady *et al*., 2020)**. Coagulation-flocculation using aluminum derivatives was found to be effective in removing pollutants from the Nile River **(El-Awady *et al*., 2015)**. Integrated treatment methods for recycling industrial wastepaper using zero liquid discharge (ZLD) and solar energy were developed by **El-Awady *et al*. (2019)** to address water shortages and energy conservation. Additionally, **El-Awady *et al*. (2017)** found that secondary treated effluent from wastewater treatment plants had no mutagenicity or cytotoxicity effects and was suitable for various agricultural activities.

Metal-organic frameworks (MOFs) are a type of crystalline material consisting of metal ions or clusters linked by organic ligands. Due to their high surface area, tunable pore sizes and chemical stability, MOFs have attracted significant attention for various applications, including water treatment, pesticide removal and reclamation **(Mohan *et al*., 2023)**. Among the various MOFs, iron-based metal-organic frameworks (Fe-MOF nanoparticles) showed great potential for water reclamation due to their unique structure and superior adsorption properties for a wide range of pollutants. The synthesis, structure and current technologies for water reclamation using Fe-MOF nanoparticles have been studied, providing a deep insight into the framework's integrity and its effectiveness in water treatment **(Joseph *et al*., 2021)**. Consequently, Fe-MOF nanoparticles exhibit high chemical stability, which makes them a promising candidate for long-term usage in wastewater treatment.

The expansion of highly invasive mosquitoes species has been driven by factors such as globalization, climate change and human mobility, resulting in the emergence of deadly diseases that may lead to epidemics or pandemics **(Dhimal *et al*., 2015; Ramalho *et al*., 2020)**. Among these invasive organisms, mosquitoes (Diptera: Culicidae) were particularly important vectors of various harmful pathogens and parasites, with *Anopheles, Aedes* and *Culex* being the most problematic, causing diseases such as malaria, dengue, yellow fever, filariasis, Japanese encephalitis and Zika (**Saxena *et al*., 2016)**. To control mosquito-borne diseases, a range of approaches including behavioral, chemical, biological, and mechanical methods are being used with varying degrees of success. However, the increasing insecticide resistance in mosquito vectors was recorded by **Benelli *et al*. (2016)**. Given these challenges, mosquito control programs must develop new approaches for an effective control to meet the requirements of public health. Fe-MOF nanoparticles are known as biocompatible and recyclable materials **(Christodoulou *et al*., 2023; Zhang *et al*., 2023)**. They are used as pigments, catalysts, sensors, biomedical materials and environmental pollutant cleanup agents **(Abdelhamid & Mathew 2022; Alprol *et al*., 2023; Vodyashkin *et al*., 2023)**. Various physical and chemical synthesis approaches were used to create Fe-MOF **(Abdelhameed & Abdel-Gawad, 2022; Silva *et al*., 2022; Zuliani *et al*., 2023)**. For biomedical and biological applications, synthesized Fe-MOF should have a narrow size distribution and be coated with a biocompatible material **(He *et al*., 2021; Lin and Lin, 2021; Al-Sharabati *et al*., 2022)**. To our knowledge, no data are available on the efficacy of Fe-MOF against the mosquito species *Culex pipiens*. This study aimed to assess the larvicidal efficiency of Fe-MOF nanoparticles against *Cx. pipiens* L. (Diptera: Culicidae) and its potential impact on wastewater treatment for disinfection purposes.

MATERIALS AND METHODS

Chemicals

2-aminoterephthalic acid (99%, Aldrich), ferrous chloride ($FeCl_2$, 99.9%, Aldrich), DMF (N, N-dimethylformamide, 99.9%, Aldrich), methanol (PA, Fisher Scientific) and ethanol (99.9%, Aldrich) were used.

Synthesis of Fe-MOF nanoparticles

Fe-MOF nanoparticles were synthesized as follows: $FeCl_2$ (1.0 g, 3.38 mmol) and 2-aminoterephthalic acid (1 g, 5.5 mmol) were dissolved in 10mL DMF at room temperature. The resulting mixture was sealed and heated at 110°C for 24 hours. The yield was filtered and washed with DMF to remove any unreacted organic molecules. The product was washed with methanol to exchange with DMF and produce monodispersed Fe-MOF nanoparticles. The final product was dried in an oven at 80°C for 4 hours and then stored under vacuum before initial use.

Characterization of Fe-MOF nanoparticles

The morphological structures of the Fe-MOF nanoparticles were examined using high-resolution scanning electron microscopy (HRSEM Quanta FEG 250 with field emission gun, FEI Company, Netherlands). The elemental analysis was conducted using energy-dispersive X-ray spectroscopy (EDX). The analyzing unit (EDAX AME-TEK analyzer) was attached to the same microscope. The x-ray diffraction (XRD) was performed on the samples using an XRD, X'Pert PRO PAN analytical diffract meter (Cu Kα X-radiation at 40 kV, 50 mA, and $\lambda = 1.5406$ Å) at room temperature. Diffraction data were collected in the 2θ° range of 4°–50°, with a step size of 0.02° and a scanning rate of 1 s.

Insect collection and colony maintenance

Early third instar larvae of *Culex pipiens* were collected from two breeding sites located in Bereket Al-Hag, El-Marg, Al Qalyubia Governorate, Egypt [(L1; 30°10'20.6"N 31°23'04.2"E and L2 (Fig. 1); 30°09'59.0"N 31°22'50.5"E (Fig. 2)] during September-October 2022. The larvae were morphologically identified using standard identification keys by **Badawy *et al*. (2013)**. Third-instar larvae were individually transferred using a 3ml- plastic pipette into separate plastic containers, filled with distilled water and supplemented with fish food pellets named Tetra-Min, Germany. The larvae were maintained at a temperature of 27±2˚C, relative humidity of 70%-80%, and a photoperiod of 1:1 (L:D) hours, following the methods modified by **Farag *et al*. (2021)**.

Larvicidal bioassay

Early third-instar larvae of *Cx. pipiens* were collected and cultured as previously described. The larvicide bioassay was conducted using different concentrations of Fe-MOF nanoparticles. It was dissolved in distilled water to prepare stock solutions with different concentrations. Five different concentrations were tested in the bioassay: 10, 50, 100, 150 and 200 ppm, respectively. The untreated group was also included, which received distilled water free from chemical larvicides. Twenty-five larvae were randomly selected and transferred to plastic cups containing different concentrations of the Fe-MOF nanoparticles or distilled water in the case of the untreated group. Three replicates were used for each tested concentration. The experiment was conducted at a temperature of 27±2˚C, relative humidity of 70%-80% and a photoperiod of 1:1 (L:D) hours. The mortality of larvae was recorded after exposure at 24, 48, and 72 hours. A larva was considered dead when it did not show any response when prodded using a fine brush. The percentage mortality was calculated for each concentration. The data were analyzed using the probit analysis method according to **Finney (1971)** to calculate the lethal concentrations (LC_{50} and LC_{95}). The slope of the concentration-response curve was estimated using regression analysis. The significance of the results was determined using the statistical software SPSS version 25.

Transmission electron microscope (TEM) studies

The midgut of 3rd *Cx. pipiens* and the ovary of adult *Cx. pipiens* that were treated with Fe-MOF nanoparticles were observed using TEM after 48 hours of treatment. The larvae, both treated and untreated, were prepared following the methodology of **Disbrey and Rack (1970)**. Ten larvae and ten adults were selected for each treatment and placed in a 1.5% (v/v) glutaraldehyde solution in 0.1 M phosphate buffer (pH 7.2) for 48 hours at 4°C. The samples were dehydrated using a series of ethanol solutions and embedded in araldite. The abdominal integument was examined using a light microscope after staining with toluidine blue, while ultrathin sections (0.1 µm) were stained with uranyl acetate and lead citrate before being analyzed microscopically using TEM (JEOL 1000, Japan) at the Electron Microscope Unit, Central Laboratory, National Research Center Giza, Egypt.

Treatment of raw drainage wastewater samples

Drainage raw wastewater samples were collected from two different locations [L1; 30°10'20.6"N 31°23'04.2"E (Fig. 1) and L2; 30°09'59.0"N 31°22'50.5"E (Fig. 2)] for the purpose of disinfection and destruction of infested areas with larvae and adult mosquitoes. The samples were labeled as follows: L1= Raw wastewater from location one; T1= Treated wastewater from location one using Nano-Fe-MOF nanoparticles; L2= Raw wastewater from location two, and T2= Treated wastewater from location two using Nano-Fe-MOF nanoparticles. The samples were analyzed for multiple parameters including pH, turbidity (NTU), total solids (TS), total dissolved solids (TDS), total suspended solids (TSS), chemical oxygen demand (COD), phosphate (PO_4), total Kjeldahl nitrogen (TKN), total alkalinity (T. Alk), total hardness (TH), nitrate (NO_3), nitrite (NO_2), chloride (Cl^-), sulfate (SO_4^{--}), chromium (Cr), cadmium (Cd) and lead (Pb), respectively. The experiments were performed in triplicate, and all analyses were carried out according to the American Standard Methods for Water and Wastewater **(APHA, 2017)**.

In this experiment, aluminum solutions were tried for chemical treatment. Poly-aluminum chloride (PAC) fulfilled the best removal results of the applied coagulants. Twenty mg of poly aluminum chloride (PAC) was added to 1 Liter wastewater samples. The jar test (Fig. 3) was used to detect the optimal experimental conditions for the reaction. The treatment removal efficiencies were calculated according to the following equation:

$$\eta = \frac{C_o - C_t}{C_o} \text{ x } 100\%$$

Where, η represents the removal efficiency for sulfate or other ions; Co and Ct are the initial and final concentrations mg/L, respectively.

Fig. 1. Location of first wastewater sample L1 at 30°10'20.6"N 31°23'04.2"E.

Fig. 2. Location of second wastewater sample L2 at 30°09'59.0"N 31°22'50.5"E.

Jar-test experiment

In this technique, as shown in Fig. (3), poly-aluminum chloride (PAC) was chosen as a selected coagulant to treat all raw industrial wastewater as well as the treated samples. PAC agglomerated the fine suspended solids and organic matters to form coarse particulates that are easily settled due to their weights. A series of experiments were performed to reach optimal operating conditions. To detect the optimal operating conditions like pH, coagulant dose, coagulant-aid dose and settling time. At optimal conditions, the PAC dose was added within the flash mixing, followed by flocculation stages and was then left to settle. After the relevant settling time, the supernatant was frequently aspirated and examined for treatment efficiency. Both NTU and chemical oxygen demand were examined for supernatant in the jars, while sludge quality including its volume, weight, and compaction were checked at optimal conditions.

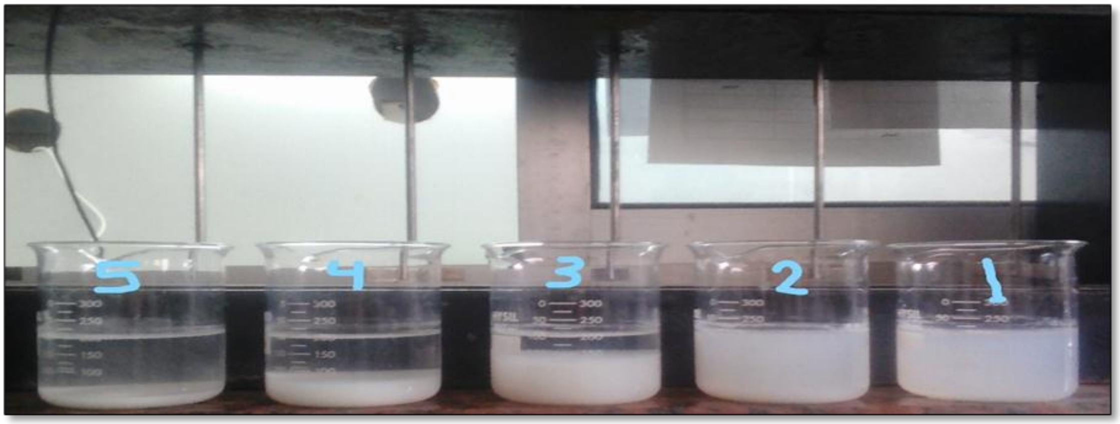

Fig. 3. Jar test experiment using poly aluminum chloride (PAC) detecting the optimal operating conditions for industrial wastewater treatment

RESULTS

1. Characterization of Fe-MOF nanoparticles

The scanning electron microscopy (SEM) images (Fig. 4A) suggest that highly crystalline Fe-MOF nanoparticles were formed. It can be found that some long strips with 5µm size of Fe-MOF nanoparticle crystals were clearly visible, and most of them were rod and spherical shapes, which were uniformly dispersed and not aggregated. EDX analysis showed the presence of Fe^{3+}, carbon, oxygen and nitrogen in the prepared materials. Fig. (4B) investigates the powder x-ray diffraction (PXRD) patterns of Fe-MOF nanoparticles. It is obvious that all amine-modified Fe-MOF nanoparticles showed similar PXRD patterns related to those of Fe-MIL-101-NH2, which indicates that the amine-modified Fe-MOF nanoparticles were successfully synthesized and that they exhibit the same 2θ at 8.5°,10.2°, 12.4°, 15.0°, 17.4° and 26.2°, which are characterized by MIL-101-NH2 **(Xie *et al*., 2017)**.

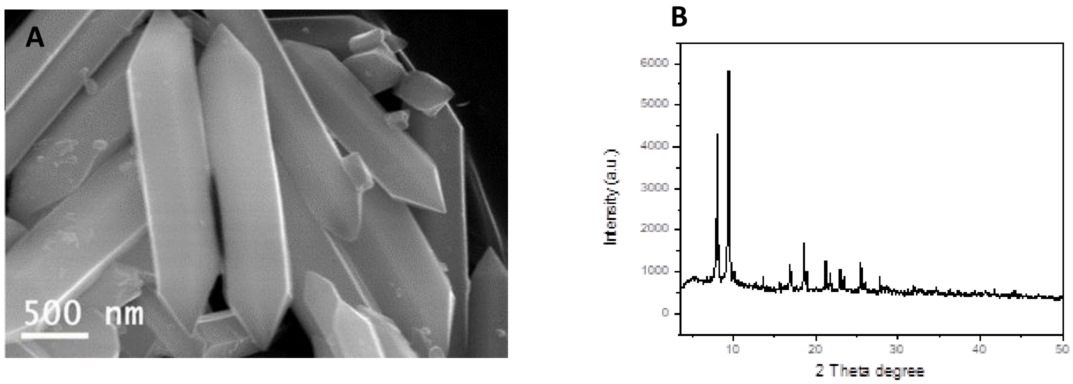

Fig. 4. SEM microphotograph of Fe-MOF nanoparticles (x= 500 nm) [A], XRD patterns of Fe-MOF nanoparticles particles [B].

2. Larvicidal bioassay

The susceptibility of 3rd instar larvae of *Cx. pipiens* to Fe-MOF nanoparticles at different time intervals and concentrations was studied, and they are recorded in Table (1). This Table shows the mortality percentages (%) of larvae at 24, 48, and 72 hours of exposure to different concentrations (10, 50, 100, 150 and 200 ppm) of Fe-MOF nanoparticles. The untreated group did not show any mortality. The LC_{50} values for iron nano compound at 24, 48, and 72 hours were 93.48, 48.68, and 40.88 ppm, respectively. The LC_{95} values at 24, 48, and 72 hours were 548.23, 293.23, and 249.28 ppm, respectively. These results indicate the toxicity of iron nano compounds on *Cx. pipiens* larvae is concentration- and time-dependent.

Table 1. Susceptibility of 3rd instar larvae of *Culex pipiens* treated with Fe-MOF nanoparticles at different time intervals and coefficient limits

Conc. ppm	**Time intervals and mortality percentages %**		
	24 hours	**48 hours**	**72 hours**
Untreated	$0.00±0^{a}$	$0.00±0^{a}$	$0.00±0^{a}$
10	$4.00± 2.1^{b}$	$9.33±0.6^{b}$	$11.67±1.4^{b}$
50	$24.00±0.9^{c}$	$48.00±6.5^{c}$	$55.00±1.7^{c}$
100	$46.66±1.2^{d}$	$70.66±1.3^{d}$	$73.33±1.5^{d}$
150	$66.66±1.1^{e}$	$82.66±1^{e}$	$92.00±1.6^{e}$
200	$82.66±0.7^{f}$	$96.00± 0.9^{f}$	$98.00± 0.5^{f}$
LC_{50} (ppm) (co. limit)	93.48 (81.29 – 107.11)	48.68 (41.07 – 56.51)	40.88 (34.05 – 47.91)
Lc_{95} (ppm) (co. limit)	548.23 (405.45 – 843.37)	293.23 (232.59 – 396.80)	249.28 (197.88 – 336.40)
Slope ± SE	2.14 ± 0.20	2.10 ± 0.16	2.09 ± 0.16

Means bearing different letters within a column are significantly different (P<0.05) ANOVA, LSD test.

3. Transmission electron microscope (TEM) studies

3.1. Culex pipiens midgut

The TEM microphotograph of the cross-sectioned midgut of the untreated *Cx. pipiens* larva (Fig. 5) showed a well-organized structure of the midgut cells. The cells appeared to be intact, with well-defined boundaries and preserved organelles. Midgut epithelium was composed of a single layer of cells that were tightly packed together. The basal surface of the cells showed a well-developed basal lamina. The cytoplasm of the cells contained a large number of mitochondria, endoplasmic reticulum and ribosomes, indicating active metabolic activity. The nuclei of the cells were oval-shaped and positioned towards the basal side. While, the midgut of *Cx. pipiens* larvae treated with Fe-MOF nanoparticles (Fig. 6) showed significant alterations in the midgut structure compared to the untreated. The midgut cells appeared to be damaged and distorted, with irregular and fragmented boundaries. The basal lamina was disrupted, and the cytoplasm showed significant changes in organelle distribution and number. The number of mitochondria was reduced, and the endoplasmic reticulum showed signs of stress and swelling. The nuclei were irregularly shaped and positioned, indicating nuclear damage.

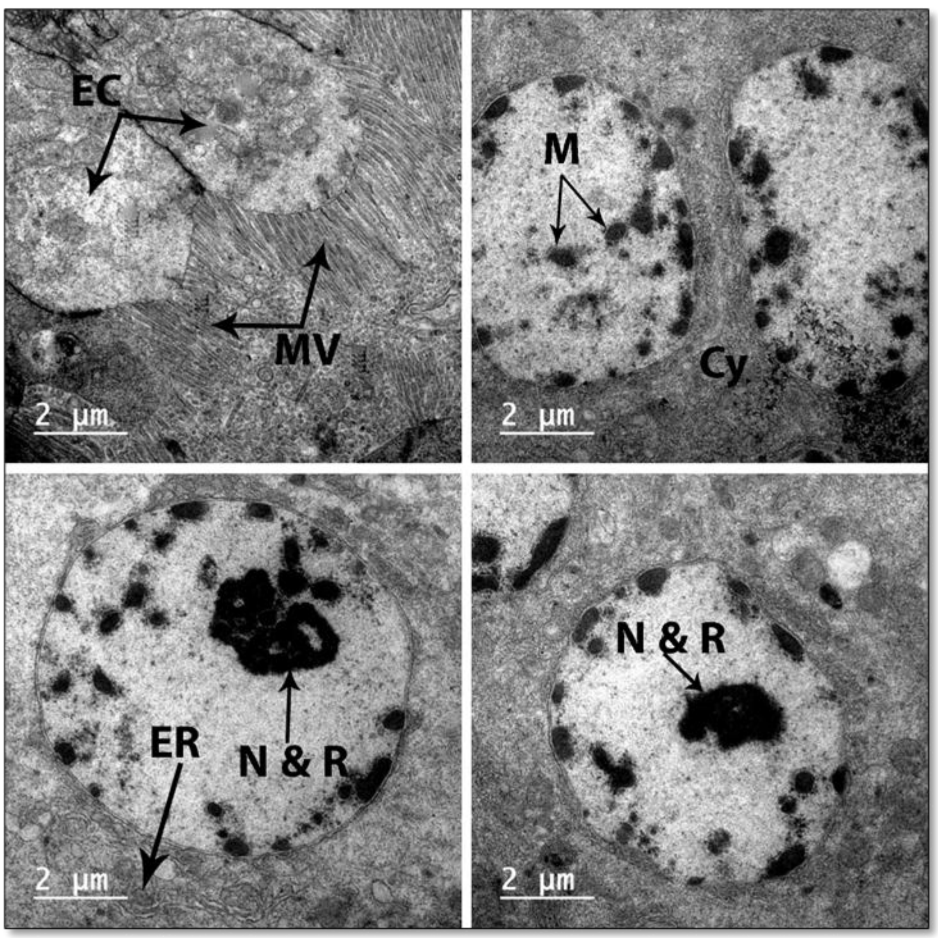

Fig. 5. Transmission electron microscopy (TEM) image of untreated midgut of *Cx. pipiens* larvae showing normal midgut epithelial cells intact to each other, epithelial cells (EC), microvilli (MV), cytoplasm (Cy), mitochondria (M), endoplasmic reticulum (ER), ribosomes (R) and normal nucleus (N).

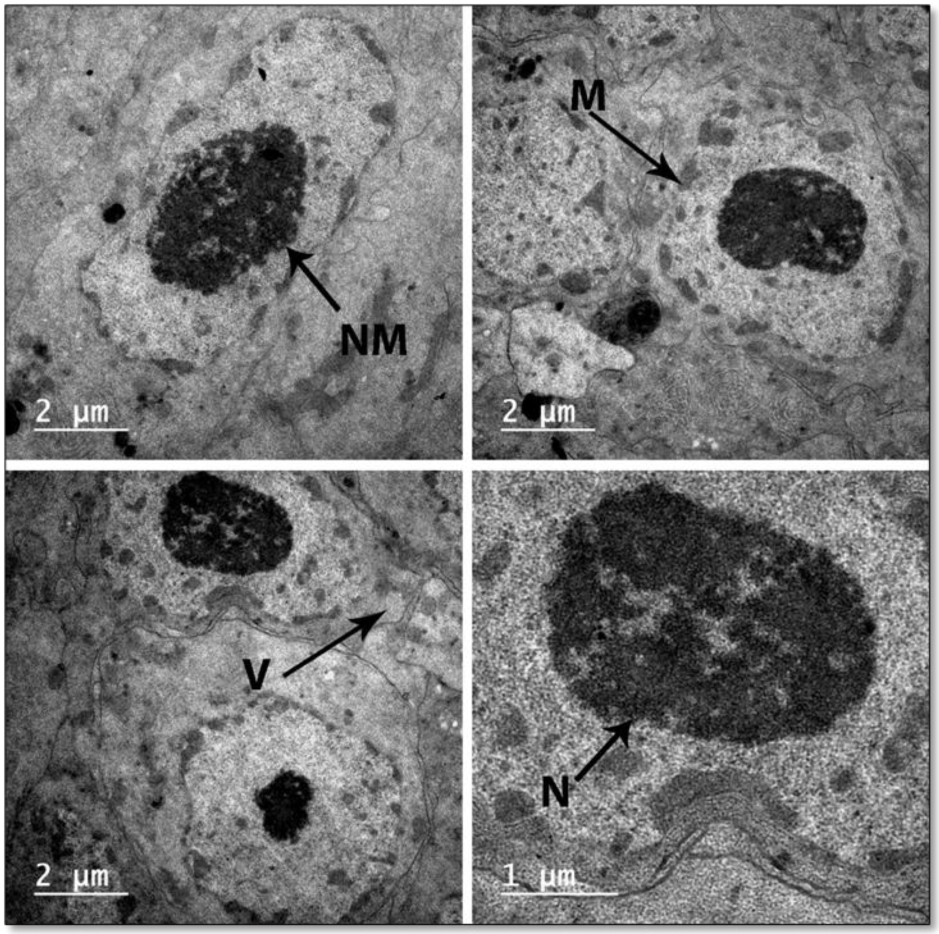

Fig. 6. Transmission electron microscopy (TEM) image of treated midgut of *Cx. pipiens* larvae with Fe-MOF nanoparticles showing abnormal nucleus (enlarged or degenerated) and unequal nuclear membrane (NM) became thinner and separated from the epidermal layer, disrupted mitochondria (M), vacuoles (V) and swollen nucleus (N).

3.2. Culex pipiens ovary

The TEM microphotograph of the cross-sectioned ovary of the untreated *Cx. pipiens* adult (Fig. 7) showed a well-organized structure of the ovarian tissue. The ovary is composed of several follicles at different developmental stages, each containing an oocyte surrounded by follicular cells. The follicular cells were tightly packed together, forming a single layer around the oocyte. The cells exhibited elongated microvilli on the apical surface, which increased the surface area for exchange between the oocyte and the surrounding environment. The basal surface of the cells showed a well-developed basal lamina. The cytoplasm of the cells contained mitochondria, endoplasmic reticulum and ribosomes, indicating active metabolic activity. The nuclei of the cells were oval-shaped and positioned towards the basal side. The oocyte showed a distinct nucleus and nucleolus, surrounded by a layer of yolk granules. The follicular cells also contained yolk granules, which were transported to the oocyte for growth and development (Fig. 7). While, those treated with Fe-MOF nanoparticles showed significant alterations in the ovarian structure, compared to the untreated control. The follicular cells exhibited irregular boundaries, and their microvilli were shortened and deformed, leading to a reduced surface area for exchange with the oocyte. The basal lamina was disrupted, and the cytoplasm showed significant changes in organelle distribution and number. The number of mitochondria was reduced, and the endoplasmic reticulum showed signs of stress and swelling. The nuclei of the follicular cells were irregularly shaped and positioned, indicating nuclear damage. The oocytes showed signs of degeneration, with a fragmented nucleus and an abnormal accumulation of yolk granules. The yolk granules were not uniformly distributed, and there was a significant reduction in their number, compared to the untreated (Fig. 8).

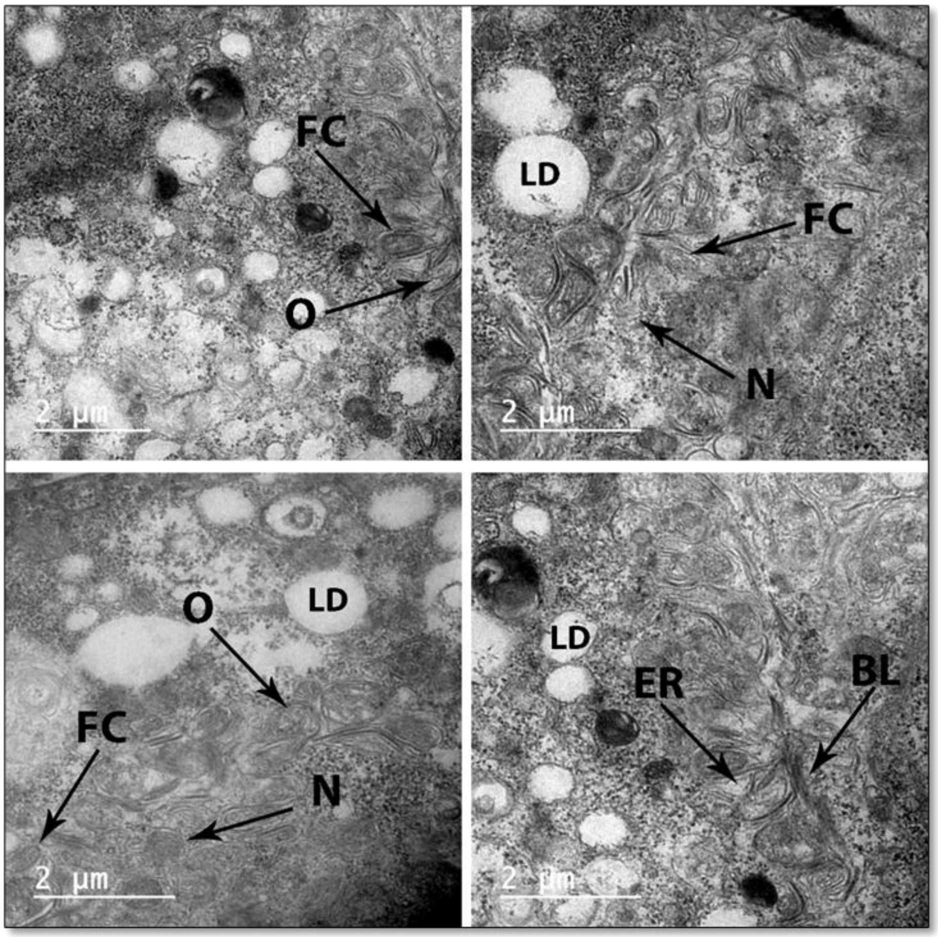

Fig. 7. Transmission electron microscopy (TEM) image of the ovary of untreated *Cx. pipiens* adults showing ovary composed of several follicles at different developmental stages, each containing an oocyte (O) surrounded by follicular cells (FC) envolved by basal lamina (BL). The follicular cells were tightly packed together, the cytoplasm of the cells contained lipid droplets (LD) and endoplasmic reticulum (ER). The oocyte showed a distinct nucleus (N) surrounded by a layer of yolk granules.

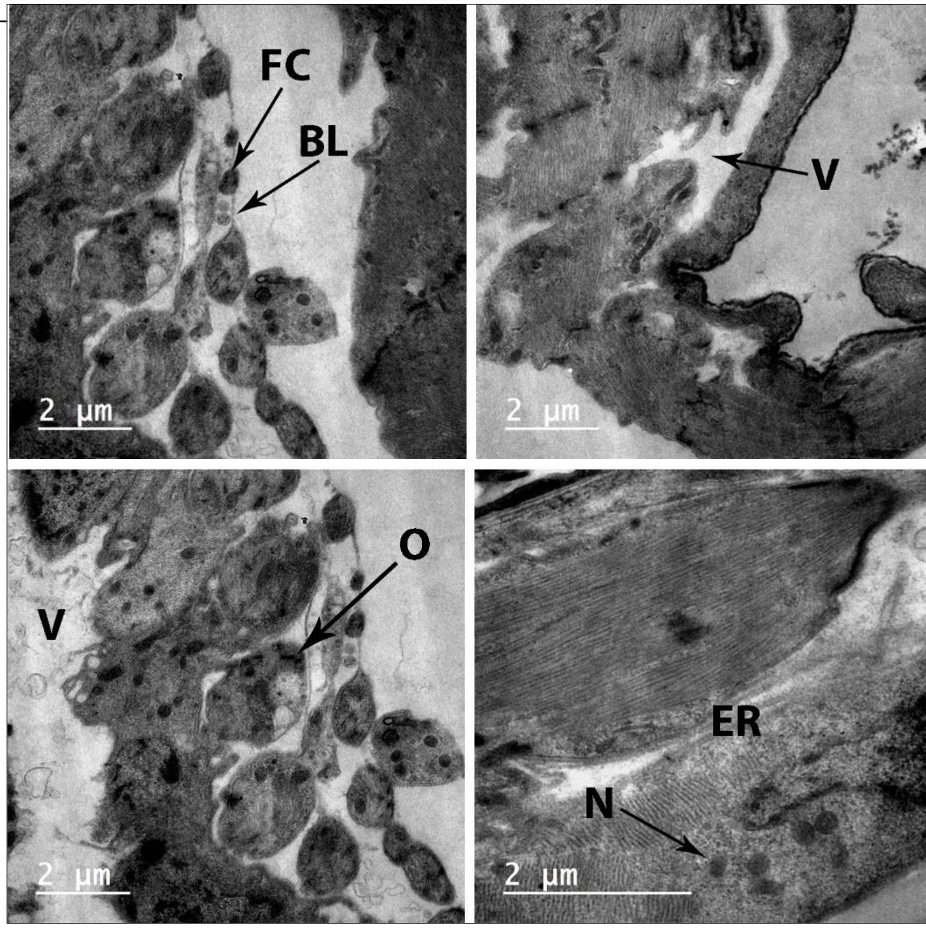

Fig. 8. Transmission electron microscopy (TEM) image of the ovary of treated *Cx. pipiens* adults with Fe-MOF nanoparticles showing follicular cells (FC) with irregular boundaries, disrupted basal lamina (BL), vacuoles (V) in the cytoplasm. Swollen endoplasmic reticulum (ER), irregular nuclei of the follicular cells (FC), degenerated oocytes (O) with a fragmented nucleus (N) and a significant reduction in the numbers and abnormal accumulation of yolk granules, compared to the untreated**.**

4. Treatment of raw drainage wastewater samples with Fe-MOF nanoparticles

The results of raw drainage wastewater L1 and L2 and the treated samples with Fe-MOF nanoparticles (T1 and T2) are presented in Table (2). The pH-values of the raw and treated samples range from 7.6 to 7.68, which are all within the acceptable safe range for discharging into the environment. The turbidity (NTU) of the treated wastewater samples had a noticeable increase from 241 to 163, compared to the raw wastewater (L1 and L2), with values of 73.8 and 152, respectively. This increase was due to the addition of Fe-MOF nanoparticles for destructing the infection in raw samples. The total solids (TS), total dissolved solids (TDS), and total suspended solids (TSS) of the raw and treated samples are almost within the same range. Moreover, the values of chemical oxygen demand (COD) of raw and treated samples are almost very close. The concentration of phosphate (PO4) in both raw and treated wastewater samples wasn't affected by the addition of iron-nanoparticles doses. The nitrogen content represented as TKN, NO3 & NO2 in raw and Fe-nano treated samples lie in the same range. Total alkalinity &

hardness for raw and treated Fe-nano particles have the same values, and the treatment didn't affect their values. In addition, the values of both chloride and sulfate in all samples have the same concentration. Results show that the concentrations of heavy metals including chromium, cadmium, lead, mercury, silver, copper, nickel, stannous and arsenic were below the detection limit in all raw and Fe-nano treated samples.

Table 2. Physico-chemical analyses of the raw drainage wastewater samples, compared to treated samples using Fe-MOF nanoparticles *

Parameter **	Unit	Results *			
		L1	T1	L2	T2
pH	-	7.6	7.6	7.65	7.68
Turbidity	NTU	73.8	241	152	163
Total solids, TS	mg/L	1174	1222	1476	1410
Total dissolved solids, TDS	mg/L	1120	1120	1260	1260
Total suspended solids, TSS	mg/L	54	102	216	150
Chemical Oxygen Demand, COD	mg/L	316	387	269	258
Phosphate, PO_4	mg/L	3.0	2.5	1.7	1.5
Total Kjeldahl, TKN	mg/L	62.7	58.2	59.4	80.6
T. Alkalinity	mg/L	800	740	520	500
T. Hardness	mg/L	450	430	385	375
Nitrate, NO_3	mg/L	ND	ND	ND	ND
Nitrite, NO_2	mg/L	ND	ND	ND	ND
Chloride, Cl^-	mg/L	480	450	500	460
Sulfate, SO_4^{--}	mg/L	135	125	140	130
Chromium, Cr	mg/L	0.02	0.01	0.02	0.01
Cadmium, Cd	mg/L	< 0.001	< 0.001	< 0.001	< 0.001
Lead, Pb	mg/L	< 0.001	< 0.001	< 0.001	< 0.001
Mercury, Hg	mg/L	< 0.001	< 0.001	< 0.001	< 0.001
Silver, Ag	mg/L	< 0.01	< 0.01	< 0.01	< 0.01
Copper, Cu	mg/L	< 0.01	< 0.01	< 0.01	< 0.01
Nickel, Ni	mg/L	< 0.001	< 0.001	< 0.001	< 0.001
Stannous, Sn	mg/L	< 0.001	< 0.001	< 0.001	< 0.001
Arsenic, As	mg/L	< 0.001	< 0.001	< 0.001	< 0.001
Boron, B	mg/L	0.59	0.48	0.69	0.92

* The mentioned results represent samples before and after nanoparticulate forms, where L1 represents raw wastewater from first location (before), and T1 represents the treated wastewater from the same location (after) using Nano-Fe-MOF nanoparticles. Also, L2 represents raw wastewater from the second location (before), and T2 represents the treated wastewater from the same location (after) using Nano-Fe-MOF nanoparticles. *The results represent the average of three successive runs. **All analyses were carried out according to American Standard Methods for Water & Wastewater Analysis (APHA), 23rd Eden, 2017. ND = Not detected

Table (3) presents the results of chemical treatment of raw and nano-treated wastewater samples. The pH values of raw and treated wastewater samples were not significantly different. The chemical treatment with PAC and polymer reduced the turbidity (NTU) of the original raw sample (L1) from 73.8 to 24.1 with removal efficiency of 67.34%, while it reduced the treated sample with Nano-Fe MOF nanoparticles (T1) from 241 to 43.4 with removal efficiency of 82%. Similarly, it reduced the NTU of the raw sample (L2) from 152 to 64.1, with removal efficiency of 57.8%, while it reduced the treated sample with Nano-Fe MOF nanoparticles (T2) from 163 to 75.5, with removal efficiency of 53.7%. Consequently, COD was significantly reduced in the treated samples, with removal efficiencies ranging from 70% to 90%. In addition, the removal efficiency of TKN varied from sample to another, with removal efficiencies ranging from 0% to 100%. On the other hand, the removal efficiency of PO_4 was found to be 100% in all treated samples. Overall, these results suggest that the chemical treatment of Fe-MOF nanoparticles can be an effective method to treat wastewater, particularly in reducing turbidity and COD.

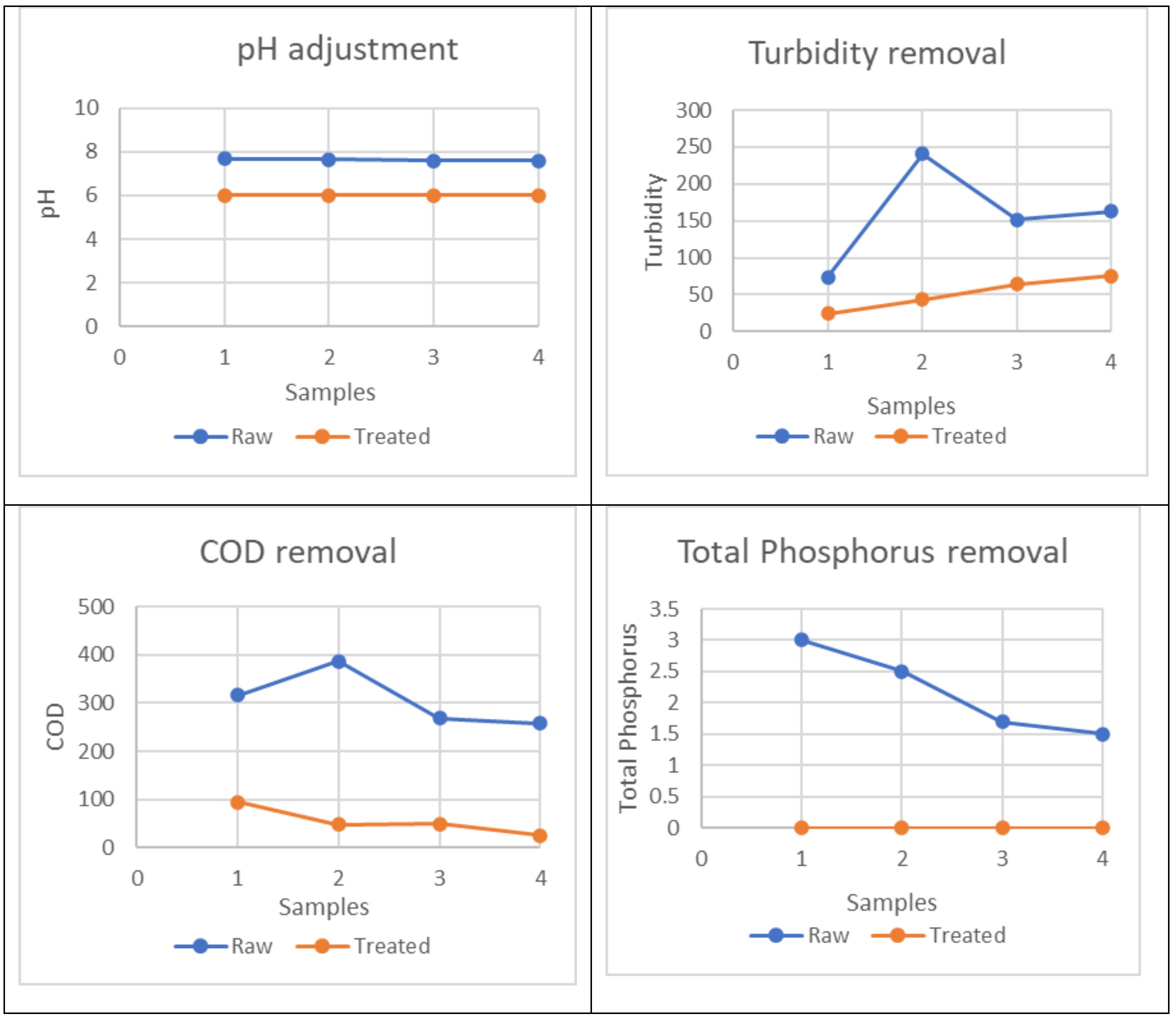

Fig. 9. Chemical treatment: pH adjustment, turbidity removal, COD removal and total phosphorus removal. The chemical treatment parameter optimization was pH at 6.0, Poly aluminum chloride (PAC) dose was 10ppm, stirring at 100rpm, and hydraulic retention time (HRT) was 30min.

Table 3. Collective chemical treatment of raw and nano-treated wastewater samples

Parameter	Unit	Results*			
		L1	T1	L2	T2
pH – value – Raw	-	7.6	7.6	7.65	7.68
pH – value – Treated		6.0	6.0	6.0	6.0
Turbidity – Raw samples	NTU	73.8	241	152	163
Turbidity – Treated		24.1	43.4	64.1	75.5
Turbidity removal efficiency	%	67.34	82	57.8	53.7
COD – Raw samples	mgO_2/L	316	387	269	258
COD – Treated		95	48	49	26
Removal efficiency	%	70	87.6	81.8	90
TKN – Raw	mg N/L	62.7	58.2	59.4	80.6
TKN – Treated		174	95	78	137
Removal efficiency	%	-	-	-	-
Phosphate, PO_4 – Raw	mg/L	3.0	2.5	1.7	1.5
Phosphate, PO_4 – Treated		0.0	0.0	0.0	0.0
Removal efficiency	%	100	100	100	100

* Average of three successive runs. *All analyses have been carried out according to American standard methods for water & wastewater analysis (APHA), 23rd Eden, 2017.

DISCUSSION

This study aimed to assess the larvicidal potentiality of Fe-MOF nanoparticles against *Culex pipiens* L. (Diptera: Culicidae) and its impact on water quality. MOFs are crystalline materials that have attracted significant attention for various applications including water treatment and reclamation **(Chen *et al*., 2019)**. Fe-MOF nanoparticles were great potential for water reclamation due to their unique structure, small droplet size and superior adsorption properties for a wide range of pollutants **(Joseph *et al*., 2021; Liu *et al*., 2023)**. The characterization of Fe-MOF nanoparticles and their potential application in wastewater treatment for disinfection purposes was invetigated in the presented study. Various analytical techniques were carried out to evaluate the morphology, structure and composition of the Fe-MOF nanoparticles, as well as the efficiency of their application in treating wastewater samples. It was found that the Fe-MOF nanoparticles are highly crystalline with a similar structure. The characterization of the prepared Fe-MOF nanoparticles in this study proved that the mean droplet size for Fe-MOF nanoparticles was 5µm, which was within the nano-size range according to **Mcclements and Rao (2011)**. The presence of Fe^{3+}, carbon, oxygen, and nitrogen in the prepared materials was confirmed by EDX analysis, while the PXRD patterns showed that the amine-modified Fe-MOF nanoparticles were successfully synthesized, exhibiting the same characteristics as MIL-101-NH_2 by **Gecgel *et al.* (2019)**, who state that photocatalysis using metal-organic frameworks (MOFs) has emerged as a promising method for the degradation of organic pollutants in an aqueous solution. Moreover, **Bedia *et al*. (2019)** emphasized the photocatalytic performance of MOFs in the purification of water and discussed the degradation of organic pollutants, such as dyes and pharmaceuticals, as well as the removal of heavy metal ions using MOF-based photocatalysts. MOFs with a very large surface area, tunable porosity, tailorable topology, crystallinity, adjustable functionalities, excellent photoelectronic properties and high thermal and mechanical stability could eradicate prevailing challenges to help water treatment **(Feng *et al*., 2018)**. Similar observations were reported by **Grover *et al.* (2010)** and **Guo *et al.* (2013)** who stated that, hematite (Fe_2O_3) nanoparticles (HNPs) might act as environmental indicators. Their results demonstrated that HNPs could be applicable in water treatment technology for the removal of metals. It was determined that different forms of iron oxide nanoparticles coated with polystyrene could help in the removal of organochlorines from aqueous solutions **(Jing *et al.* 2013)**.

The expansion of highly invasive species such as mosquitoes has led to the emergence of deadly diseases that can lead to epidemics or pandemics **(Dahmana & Mediannikov, 2020; Aly *et al.*, 2023)**. The larvicide bioassay was conducted using different concentrations of Fe-MOF nanoparticles dissolved in distilled water. The results showed that Fe-MOF nanoparticles have a larvicidal effect against *Cx. pipiens*, with a mortality rate of 98% at the highest concentration tested (200 ppm) 72 hours post-treatment. The toxic effect of Fe-MOF nanoparticles on the 3rd instar larvae of *Cx. pipiens* was significantly increased with the increase in concentration of the tested compound, indicating its potential as a larvicide. In recent times, there has been a growing interest in the use of metal nanoparticles for mosquito control purposes. These nanoparticles have shown significant potential for exhibiting toxic effects against mosquitoes throughout their various life stages **(Blore *et al*., 2022)**. **Baghela and Kachhwaha (2021)** declared that the green synthesis of copper, zinc and silver nanoparticles has shown their toxic effects against mosquitoes. Previous studies indicate that iron and iron oxide nanoparticles have a detrimental impact on *Culex quinquefasciatus*, likely due to their toxic properties. These nanoparticles may disrupt various physiological processes or cause direct damage to the mosquito larvae, leading to reduced survival or impaired development. On the other hand, the study suggests that the application of iron and iron oxide nanoparticles for mosquito control may have minimal non-target effects on these beneficial fish species **(Murugan *et al*., 2018)**. Moreover, in a previous study, the efficacy of silver nanoparticles was assessed against the larvae and pupae of two mosquito species, *Aedes albopictus* and *Culex pipiens pallens*, following different treatment durations (24, 48 and 72 hours). The findings of that study revealed that the silver nanoparticles demonstrated significant effectiveness against both mosquito species at different developmental stages **(Fouad *et al*., 2018)**. **Gunathilaka *et al*. (2021)** observed that the development rate of surviving mosquito larvae was delayed when exposed to ZnO nanoparticles, indicating their potential to both kill and inhibit the growth of *Aedes albopictus* and *Anopheles vagus* larvae. The mode of action of Fe-MOF nanoparticles on *Cx. pipiens* larvae was investigated using transmission electron microscopy. Through the ultrastructure study, the treated larvae with Fe-MOF nanoparticles showed a very different profile from the normal structure of the midgut and the ovary. The results showed that treatment with Fe-MOF nanoparticles led to significant alterations in the midgut and ovarian structures, including damage to the midgut cells and distortion of their boundaries, disrupted basal lamina, and changes in organelle distribution and number. The number of mitochondria was reduced, and the endoplasmic reticulum showed signs of stress and swelling. The nuclei of the cells were irregularly shaped and positioned, indicating nuclear damage. The changes that were observed in the midgut cells are explained by the fact that this portion of the digestive tract, which is responsible for digestion in insects, is in direct contact with the toxic elements, causing death, as stated by **Ga'al *et al*. (2018)**. The afore- mentioned authors reported that the histological analysis of the midgut cells of the untreated and treated larvae revealed that the epithelial cells and brush border were highly affected by the silver nanoparticles synthesized using *Aquilaria sinensis* and *Pogostemon cablin* essential oils against the *Aedes albopictus* mosquito. Histopathological studies by **Wilson *et al.* (2022)** showed that, the cellular level of the midgut area was highly affected by using green synthesized AgNPs applied to *Aedes aegypti*, *Anopheles stephensi,* and *Culex quinquefasciatus*. On the same line, **Yasur and Rani (2015)** studied the toxicity of silver nanoparticles on two lepidopteran pests and reported severe damage in the midgut epithelium of the treated larvae and the accumulation of silver nanoparticles in cell organelles. In the same context, **Morsy *et al.* (2022)** reported the effect of silver nanoparticles against black cutworm (*Agrotis ipsilon*) larvae and revealed that there was clear damage to the epithelial cells of the midgut. The follicular cells in the ovary exhibited irregular boundaries, shortened and deformed microvilli, a disrupted basal lamina and significant changes in organelle distribution and number. The oocytes showed signs of degeneration, with a fragmented nucleus and an abnormal accumulation of yolk granules. The results suggest that Fe-MOF nanoparticles have a distortion effect on the midgut and ovarian tissues of *Cx. pipiens* larvae, potentially disrupting metabolic activity and causing structural damage. Moreover, the study found that Fe-MOF nanoparticles did not have any adverse effects on water quality parameters such as pH, dissolved oxygen and turbidity. Therefore, MOF-Fe could be considered a safe and effective alternative for controlling mosquito-borne diseases. The efficient properties of nanopesticides as a tool for vector control can be attributed to their nanometric size, which allows for easier passage into cells. The small size below 100nm facilitates their penetration into host cells, making their application specific to different nanopesticides and hindrance mechanisms. Metallic nanoparticles hinder the molecular level by targeting DNA and RNA, ultimately leading to host mortality **(Mishra *et al*., 2018)**. The findings of this study could contribute to the development of new approaches for mosquito control programs that meet the requirements of public health. Similar results were reported by **Nasr-Eldahan *et al*. (2021)** who found that, nanoparticles have no adverse effect on water quality and have no toxic effect on non-target organisms like fish.

Regarding the application of Fe-MOF nanoparticles in wastewater treatment, the efficiency of the treatment was evaluated by analyzing the chemical and physical properties of the raw and nano-treated wastewater samples. It was found that significant improvements in the quality of the treated wastewater were achieved by the application of Fe-MOF nanoparticles, as indicated by the reduction in turbidity, total solids, chemical oxygen demand (COD) and other parameters. The removal efficiency of turbidity was found to be as high as 82%, while the removal efficiency of COD was up to 95%. These results indicate that Fe-MOF nanoparticles can be an effective solution for treating wastewater and reducing the concentration of pollutants. Similar observations were reported by the work of **Crispim *et al*. (2022)** when they applied electro-Fenton (EF) and photoelectro-Fenton (PEF) for treating a local landfill effluent with high organic content and high chemical oxygen demand (COD), with a removal proficiency of 89%. The importance of metal oxide nanoparticles in wastewater purification was recorded in previous studies, such as **Khan *et al.* (2013)**, **Feng *et al.* (2018)**, **Subudhi *et al.* (2018)** and **Divya and Oh (2002)**.

Overall, this study focused on evaluating the larvicidal efficacy of Fe-MOF nanoparticles against *Culex pipiens* L. mosquitoes and assessing their impact on water quality. The results demonstrated that Fe-MOF nanoparticles possess significant larvicidal activity against *Cx. pipiens* larvae, leading to a high mortality rate. The present results agree with those of **Mahmoud *et al*. (2022)**, **Vasseghian *et al*. (2022)**, **Nie *et al*. (2023)** and **Yin *et al*. (2023)** who reported that, Fe-MOF nanoparticles are effective insecticidal agents against different species of insects. The absorbance of nanoparticles into the cuticular lipids of the insects results in the destruction of the protective wax layer **(Benelli, 2018; Mahmoud *et al.*, 2022)**. Additionally, the study investigated the potential structural damage caused by Fe-MOF nanoparticles in the midgut and ovarian tissues of the treated larvae. The obtained results agree with those **Vecchio *et al.* (2013)** who found that, iron oxide nanoparticles were highly toxic, displaying a 30% viability reduction in *Drosophila melanogaster* at low concentrations, and with those of **Chen *et al.* (2014)** who reported that the application of three types of iron oxide nanoparticles against *Drosophila melanogaster* caused an obvious reduction in female fecundity, and developmental delay at the egg-pupae and pupae-adult transitions. Further investigations indicated that the paternal uptake of nanoparticles disturbed the oogenesis period, induced ovarian defects, reduced the length of eggs, affected the number of nurse cells and delayed egg chamber development.

These findings contribute to our understanding of Fe-MOF nanoparticles as a promising larvicide for effectively controlling *Cx. pipiens* mosquitoes. Moreover, the study highlights the importance of considering the impact of larvicidal agents on water quality, emphasizing the need for sustainable and environmentally friendly approaches in mosquito control programs.

CONCLUSION

From the current study, it can be concluded that Fe-MOF nanoparticles showed significant improvements in the quality of the treated wastewater samples. Fe-MOF nanoparticles show potential as a safe and effective alternative for controlling mosquito-borne diseases, offering a promising strategy for mosquito population control and disease prevention.

ETHICAL APPROVAL

This research paper was approved by the research ethics committee from the Faculty of Science, Ain Shams University (ASU-SCI/ENTO/2023/5/3).

REFERENCES

Abdelhameed, R.M. and Abdel-Gawad, H. (2022). Metal organic frameworks (MOFs) based 2-Amino-1,4-Benzenedicarboxylic acid linker: Synthesis and post-synthetic modification. Egypt. J. Chem., 65(6): 453-475.

Abdelhamid, H.N. and Mathew, A.P. (2022). Cellulose metal organic frameworks (CelloMOFs) hybrid materials and their multifaceted Applications: A review. Coord. Chem. Rev., 451: 214263.

Aly, S.H.; Elissawy, A.M.; Salah, D.; Alfuhaid, N.A.; Zyaan, O.H.; Mohamed, H.I.; Singab, A.N.B. and Farag, S.M. (2023). Phytochemical investigation of three *Cystoseira* species and their larvicidal activity supported with in silico studies. Mar. Drugs, 21:117.

Al-Sharabati, M.; Sabouni, R. and Husseini, G.A. (2022). Biomedical applications of metal organic frameworks for disease diagnosis and drug delivery: A Review. Nanomaterials, 12(2): 277.

Alprol, A.E.; Mansour, A.T.; Abdelwahab, A.M. and Ashour, M. (2023). Advances in green synthesis of metal oxide nanoparticles by marine algae for wastewater treatment by adsorption and photocatalysis techniques. Catalysts, 13:888.

APHA (2017). Standard methods for the examination of water and wastewater (23rd ed.). Washington DC: American Public Health Association.

Badawy, R.M.; Hoseny, I.M. and Talal, M. (2013). Biodiversity and seasonal fluctuation of aquatic and semiaquatic insects in Rashid stream, kafr El Zayat (Gharbyia governorate). Egypt. Acad. J. Biolog. Sci., 6(1): 47-66.

Baghela, V. and Kachhwaha, N. (2021). Efficacy of nanoparticles as a research tool to control mosquito vector. A Review. Flora and Fauna, 27(2): 271-278.

Bagheri, A.R.; Aramesh, N. and Bilal, M. (2021). New frontiers and prospects of metal-organic frameworks for removal, determination, and sensing of pesticides. Enviro. Res., 194: 110654.

Bedia, J.; Muelas-Ramos, V.; Penas-Garzon, M.; Gomez-Aviles, A.; Rodriguez, J.J. and Belver, C. (2019). A review on the synthesis and characterization of metal organic framework for photocatalytic water purification. Catalysts, 9 (1): 52.

Benelli, G. (2018). Mode of action of nanoparticles against insects. Environ Sci Pollut Res Int. 25(13):12329-12341.

Benelli, G.; Jeffries, C. L. and Walker, T. (2016). Biological control of mosquito vectors: Past, present, and future. Insects, 7: 52.

Blore, K.; Baldwin, R.; Batich, C.D.; Koehler, P.; Pereira, R.; Jack, C.J.; Qualls, W.A. and Xue, R.D. (2022). Efficacy of metal nanoparticles as a control tool against adult mosquito vectors: A review. Frontiers in Tropical Diseases, 3:969299.

Chen, D.; Feng, P. and Wei, F. (2019). Preparation of Fe (III)-MOFs by microwave-assisted ball for efficiently removing organic dyes in aqueous solutions under natural light. Chem. Eng. Process. Process Intensif., 135: 63-67.

Chen, H.; Wang, B.; Feng, W.; Du, W.; Ouyang, H.; Chai, Z.; and Bi, X. (2014). Oral magnetite nanoparticles disturb the development of *Drosophila melanogaster* from oogenesis to adult emergence. Nanotoxicology, 5390:1–11.

Chowdhary, P.; Bharagava, R. N.; Mishra, S. and Khan, N. (2020). Role of industries in water scarcity and its adverse effects on environment and human health. Environ. Concerns Sustain. Dev., 235–256.

Christodoulou, I.; Lyu, P.; Soares, C.V.; Patriarche, G.; Serre, C.; Maurin, G. and Gref, R. (2023). Nanoscale Iron based metal organic Frameworks: Incorporation of Functionalized Drugs and Degradation in Biological Media. Int. J. Mol. Sci., 24: 3362.

Crispim, A.C.; de Araújo, D. M.; Martínez-Huitle, C. A.; Souza, F.L. and Dos Santos, E. V. (2022). Application of electro-Fenton and photoelectro-Fenton processes for the degradation of contaminants in landfill leachate. Enviro. Res., 213: 113552.

Dahmana H. and Mediannikov, O. (2020). Mosquito-borne diseases emergence resurgence and how to effectively control it biologically. Pathogens, 9(4):310.

Dhimal, M.; Ahrens, B. and Kuch, U. (2015). Climate change and spatiotemporal distributions of vector-borne diseases in Nepal—A systematic synthesis of literature. *PLoS ONE*, 10: e0129869.

Disbrey, B.D. and Rack, J.H. (1970). Histological laboratory methods. E & S Livingstone, Edinburgh.

Divya, S. and Oh, T.H. (2022). Polymer nanocomposite membrane for wastewater treatment: A Critical Review. Polymers, 14(9): 1732.

El-Awady, M.; Hamza, S.M.; Mangood, A.H. and Soliman, A.A. (2015). Optimal coagulation/flocculation process for water treatment plants located on Damietta branch of

River Nile, Egypt. International Journal of Technology Enhancements and Emerging Engineering Research, 3: 71-77.

El-Awady, M.H. and Ali, S.A. (2012). Nonconventional treatment of sewage sludge using cement kiln dust for reuse and catalytic conversion of hydrocarbons. *Environmentalist*, 32: 464-475.

El-Awady, M.H.; Ahmed, M.A. and Dahaba, A. (2020). Sulfate reduction and heavy metals removal from industrial wastewater via advanced calcium-aluminum precipitation method. Egypt J. Chem., 63(5): 1897-1912.

El-Awady, M.H.; El-Ghetany, H.H.; Aboelghait, K.M. and Dahaba, A.A. (2019). Zero liquid discharge and recycling of paper mill industrial wastewater via chemical treatment and solar energy in Egypt. Egypt J. Chem., 62: 37-45.

El-Awady, M.H.; Marzouk, N.M.; Bakry, B.A.; Rahman, H.M.A. and Kenawy, A. (2017). Treated wastewater impact on rural green farm life cycle, Egypt. Egypt. J. Chem., 60(6): 965-975.

Farag, S.M., Hussein, A.M., Hafez, E.S., Khaled, A.S., Kamel, O.M., Zyaan, O.H. (2021). Larvicidal, biological, and histopathological alterations induced by pomegranate peel extract, *Punica granatum* against *Culex pipiens* L. (Diptera: Culicidae). Egypt. J. Aquat. Biol. Fish., 25(2): 139-161. doi: 10.21608/ejabf.2021.160288

Feng, M.; Zhang, P.; Zhou, H.C. and Sharma, V.K. (2018). Water-stable metal-organic frameworks for aqueous removal of heavy metals and radionuclides: a review. Chemosphere, 209: 783-800.

Finney, D.J. (1971). Probit Analysis. 3rd Edition, Cambridge University Press, Cambridge.

Fouad, H.; Hongjie, L.; Hosni, D.; Wei, J.; Abbas, G.; Ga'al, H. and Jianchu, M. (2018). Controlling *Aedes albopictus* and *Culex pipiens pallens* using silver nanoparticles synthesized from aqueous extract of Cassia fistula fruit pulp and its mode of action. Artif. Cells Nanomed. Biotechnol., 46(3): 558-567.

Ga'ala, H.; Fouada, H.; Maoa, G.; Tiana, J. and Jianchu, M. (2018). Larvicidal and pupicidal evaluation of silver nanoparticles synthesized using *Aquilaria sinensis* and *Pogostemon cablin* essential oils against dengue and zika viruses' vector *Aedes albopictus* mosquito and its histopathological analysis. Artif. Cells Nanomed. Biotechnol., 46(6): 1171–1179.

Gecgel, C.; Simsek, U.B.; Gozmen, B. and Turabik, M. (2019). Comparison of MIL-101(Fe) and amine-functionalized MIL-101(Fe) as photocatalysts for the removal of imidacloprid in aqueous solution. J. Iranian Chem. Soc., 16: 1735–1748.

Gunathilaka, U.M.; de Silva, W.A.; Dunuweera, S.P. and Rajapakse, R.M. (2021). Effect of morphology on larvicidal activity of chemically synthesized zinc oxide nanoparticles against mosquito vectors. RSC Advances, 11: 8857-8866.

Grover, V.A.; Jinxuan, H. U., Engates, K.E. and Shipley, H.J. (2012). Nanomaterials in the environment adsorption and desorption of bivalent metals to hematite nanoparticles. Environ. Toxicol. Chem., 31(1):86-92.

Guo, H.; Xu, H. and Barnard, A.S. (2013). Can hematite nanoparticles be an environmental indicator. Energy Environ. Sci., 6:561-569.

He, S.; Wu, L.; Li, X.; Sun, H.; Xiong, T.; Liu, J.; Huang, C.; Xu, H; Sun, H.; Chen, W.; Gref, R. and Zhang, J. (2021). Metal-organic frameworks for advanced drug delivery. Acta Pharmaceutica Sinica *B*, 11(8): 2362-2395.

Jing, L.A.N.; Yang, C. and Zongshan, Z. (2013). Effective organochlorine pesticides removal from aqueous systems by magnetic nanospheres coated with polystyrene. J. Wuhan Univ. Technol.-Mat. Sci. Edit., 29(1):168–173.

Joseph, J.; Iftekhar, S.; Srivastava, V.; Fallah, Z.; Zare, E.N. and Sillanpää, M. (2021). Iron-based metal-organic framework: Synthesis, structure, and current technologies for water reclamation with deep insight into framework integrity. Chemosphere, 284: 131171.

Khan, N.A.; Hasan, Z. and Jhung, S.H. (2013). Adsorptive removal of hazardous materials using metal-organic frameworks (MOFs): a review. J. Hazard Mater., 244–245: 444-456.

Lin, Y.S. and Lin, K.S. (2021). Characterization of the size and porous temperature sensitivity of Pluronic F127–Coated MIL–88B(Fe) for drug release. Micropor. Mesopor. Mater., 328: 111456.

Liu, X.; Shan, Y.; Zhang, S.; Kong, Q. and Pang, H. (2023). Application of metal organic framework in wastewater treatment. Green Energy & Environment, 8(3): 698-721.

Mahmoud, L.A.M.; Dos Reis, R.A.; Chen, X.; Ting, V.P. and Nayak, S. (2022). Metal-organic frameworks as potential agents for extraction and delivery of pesticides and agrochemicals. ACS Omega., 7(50): 45910-45934.

Mcclements, D. and Rao, J. (2011). Food-Grade Nanoemulsions: formulation, fabrication, properties, performance, biological fate, and potential toxicity. Crit Rev Food Sci Nutr., 51(4): 285-330.

Mishra, P.; Tyagi, B.K.; Chandrasekaran, N. and Mukherjee, A. (2018). Plant-borne compounds and nanoparticles: challenges for Medicine, Parasitology, and Entomology. Environ. Sci. Pollut. Res., 25, 10151-10163.

Mohan, B.; Kamboj, A.; Virender, Singh, K.; Priyanka, Singh, G.; Pombeiro, A.J.L. and Ren, P. (2023). Metal-organic frameworks (MOFs) materials for pesticides, heavy metals, and drugs removal: Environmental safety. Sep. Purif. Technol., 310: 123175.

Morsy, A.R. Mohamed, G. R., El- Shewy A.M. (2022). The efficiency of chitosan & silver and their nanoparticles on histological and enzymatic activities of land snail, *Monacha obstructa* and Cutworm, *Agrotis ipsilon*. Egypt. Acad. J. Biolog. Sci., 14(1):159-178.

Murugan, K.; Dinesh, D.; Nataraj, D.; Subramaniam, J.; Amuthavalli, P.; Madhavan, J.; Rajasekar, A.; Rajan, M.; Thiruppathi, K.P.; Kumar, S.; Higuchi, A.; Nicoletti, M. and Benelli G. (2018). Iron and iron oxide nanoparticles are highly toxic to *Culex quinquefasciatus* with little non-target effects on larvivorous fishes. Environ Sci Pollut Res Int., 25(11):10504-10514.

Nasr-Eldahan, S.; Nabil-Adam, A. and Shreadah, M.A. (2021). A review article on nanotechnology in aquaculture sustainability as a novel tool in fish disease control. Aquacult. Int., 29: 1459–1480.

Nie, D.; Li, J.; Xie, O.; Ai, L.; Zhu, C.; Wu, Y.; Gui, Q.; Zhang, L. and Tan, W. (2023). Review Article Nanoparticles: A Potential and effective method to control Insect. Bioinorg. Chem. Appl., 6:1-13.

Ramalho-Ortigao, M. and Gubler, D. J. (2020). Human diseases associated with vectors (arthropods in disease transmission). In E. T. Ryan, D. R. Hill, T. Solomon, N. E. Aronson, & T. P. Endy (Eds.), Hunter's Tropical Medicine and Emerging Infectious Diseases (Tenth Edition) (pp. 1063-1069). Elsevier.

Saxena, S.K.; Elahi, A.; Gadugu, S. and Prasad, A. K. (2016). Zika virus outbreak: An overview of the experimental therapeutics and treatment. Virus Disease, 27: 111-115.

Silva, A.R.M.; Alexandre, J.Y.N.H.; Souza, J.E.S.; Neto, J.G.L.; de Sousa Júnior, P.G.; Rocha, M.V.P. and Dos Santos, J.C.S. (2022). The Chemistry and applications of metal-organic frameworks (MOFs) as industrial enzyme immobilization systems. Molecules, 27(14): 4529.

Subudhi, S.; Rath, D. and Parida, K.M. (2018). A mechanistic approach towards the photocatalytic organic transformations over functionalised metal organic frameworks: a review. Catal. Sci. Technol., 8: 679-696.

Vasseghian, Y.; Arunkumar, P.; Joo, S.; Gnanasekaran, L. Kamyab, H.; Rajendran, S.; Balakrishnan, D.; Chelliapan, S. and Klemes, J. (2022). Metal-organic framework-enabled pesticides are an emerging tool for sustainable cleaner production and environmental hazard reduction. Journal of Cleaner Production, 373:133966.

Vecchio, G.; Galeone, A.; Malvindi, M. A.; Cingolani, R. and Pompa, P.P. (2013). Ranking the in vivo toxicity of nanomaterials in *Drosophila melanogaster*. J. Nanoparticle Res., 15:1963.

Vodyashkin, A.A.; Sergorodceva, A.V.; Kezimana, P. and Stanishevskiy, Y.M. (2023). Metal-Organic Framework (MOF)—A Universal Material for Biomedicine. Int. J. Mol. Sci., 24: 7819.

Wilson, J.J.; Lakshmi, M.P.; Sivakumar, T.; Ponmanickam, P. and Sevarkodiyone, S.P. (2022). Green synthesis of silver nanoparticles using Bacillus subtilis (P3) and its larvicidal, histopathological and biotoxicity efficacy. S. Afr. J. Bot., 151(B): 309-318.

Xie, Q.; Li, Y.; Lv, Z.; Zhou, H.; Yang, X.; Chen, J. and Guo, H. (2017). Effective Adsorption and Removal of Phosphate from Aqueous Solutions and Eutrophic Water by Fe-Based MOFs of MIL-101. Sci. Rep., 7(1): 3316-3331.

Yasur J. and Rani P.U. (2015). Lepidopteran insect susceptibility to silver nanoparticles and measurement of changes in their growth, development, and physiology. Chemosphere, 124: 92-102.

Yin, J.; Su, X.; Yan, S. and Shen, J. (2023). Multifunctional nanoparticles and nano pesticides in agricultural application. Nanomaterials, 13:1255.

Zhang, L.; Zheng, Q.; Zhang, Z.; Li, H.; Liu, X.; Sun, J. and Wang, R. (2023). Application of metal–organic frameworks (MOFs) in environmental biosystems. Int. J. Mol. Sci., 24: 2145.

Zuliani, A.; Khiar, N. and Carrillo-Carrión, C. (2023). Recent progress of metal–organic frameworks as sensors in (bio)analytical fields: towards real-world applications. Analytical and Bioanalytical Chemistry, 415: 2005–2023.